Biomedicine & Pharmacotherapy 141 (2021) 111800

Contents lists available at ScienceDirect

Biomedicine & Pharmacotherapy

journal homepage: www.elsevier.com/locate/biopha

Inhibition of endothelin A receptor by a novel, selective receptor antagonist enhances morphine-induced analgesia: Possible functional interaction of dimerized endothelin A and μ-opioid receptors

Yui Kuroda [a,b], Miki Nonaka [b], Yuji Kamikubo [c], Haruo Ogawa [d], Takashi Murayama [c], Nagomi Kurebayashi [c], Hakushun Sakairi [c], Kanako Miyano [b,e], Akane Komatsu [a,b], Tetsushi Dodo [f], Kyoko Nakano-Ito [g], Keisuke Yamaguchi [h], Takashi Sakurai [c], Masako Iseki [a,h], Masakazu Hayashida [a,h], Yasuhito Uezono [b,h,i,j,*]

[a] Department of Anesthesiology and Pain Medicine, Juntendo University Graduate School of Medicine, Tokyo, Japan
[b] Department of Pain Control Research, The Jikei University School of Medicine, Tokyo, Japan
[c] Department of Cellular and Molecular Pharmacology, Juntendo University Graduate School of Medicine, Tokyo, Japan
[d] Institute of Molecular and Cellular Biosciences, The University of Tokyo, Tokyo, Japan
[e] Division of Cancer Pathophysiology, National Cancer Center Research Institute, Tokyo, Japan
[f] Strategy Planning & Operations, Medicine Development Center, Eisai Co., Ltd., Ibaraki, Japan
[g] Global Drug Safety, Medicine Development Center, Eisai Co., Ltd., Ibaraki, Japan
[h] Department of Pain Medicine, Juntendo University Graduate School of Medicine, Tokyo, Japan
[i] Supportive and Palliative Care Research Support Office, National Center Hospital East, Chiba, Japan
[j] Project for Supportive Care Research, Exploratory Oncology Research and Clinical Trial Center, National Cancer Center, Tokyo, Japan

ARTICLE INFO

Keywords:
Analgesic
Endothelin A receptor antagonist
G protein-coupled receptor
Morphine
Pain
Receptor heterodimerization

Chemical compounds studied in this article:
included endothelin-1 (PubChem CID: 16212950)
BQ-123 sodium salt (PubChem CID: 52943236)
BQ-788 sodium salt (PubChem CID: 23693553)
morphine hydrochloride (PubChem CID: 5464110)
and Bosentan Monohydrate (PubChem CID: 185462)

ABSTRACT

Background: The misuse of opioids has led to an epidemic in recent times. The endothelin A receptor (ETAR) has recently attracted attention as a novel therapeutic target to enhance opioid analgesia. We hypothesized that endothelin A receptors may affect pain mechanisms by heterodimerization with μ opioid receptors. We examined the mechanisms of ETAR-mediated pain and the potential therapeutic effects of an ETAR antagonist, Compound-E, as an agent for analgesia.

Methods: Real-time in vitro effect of Compound-E on morphine response was assessed in HEK293 cells expressing both endothelin A and μ opioid receptors through CellKey™ and cADDis cAMP assays. Endothelin A/μ opioid receptor dimerization was assessed by immunoprecipitation and live cell imaging. The in vivo effect of Compound-E was evaluated using a morphine analgesia mouse model that observed escape response behavior, body temperature, and locomotor activity.

Results: In CellKey™ and cAMP assays, pretreatment of cells with endothelin-1 attenuated morphine-induced responses. These responses were improved by Compound-E, but not by BQ-123 nor by bosentan, an ETAR and endothelin B receptor antagonist. Dimerization of ETARs and μ opioid receptors was confirmed by Western blot and total internal reflection fluorescence microscopy in live cells. *In vivo*, Compound-E potentiated and prolonged the analgesic effects of morphine, enhanced hypothermia, and increased locomotor activity compared to morphine alone.

Conclusion: The results suggest that attenuation by endothelin-1 of morphine analgesia may be caused by dimerization of Endothelin A/μ opioid receptors. The novel ETAR antagonist Compound-E could be an effective adjunct to reduce opioid use.

Abbreviations: ET-1, endothelin-1; ETAR, endothelin A receptor; ETBR, endothelin B receptor; MOR, μ-opioid receptor; DOR, δ- opioid receptor; KOR, κ-opioid receptor; GPCR, G protein-coupled receptor; HBSS, Hank's balanced salt solution; p.o., oral administration; s.c., subcutaneous injection; cAMP, 3′,5′-cyclic adenosine monophosphate; LDS, lithium dodecyl sulfate; DTT, dithiothreitol; HT-488, HaloTag Alexa Fluor 488 ligand; ST-594, SNAP surface 594; TIRF, total internal reflection fluorescence; CB1R, cannabinoid CB1 receptors.

* Correspondence to: Department of Pain Control Research, The Jikei University School of Medicine, 3-25-8 Nishi-Shimbashi, Minato-ku, Tokyo 105-8461, Japan.
E-mail address: yuezono@jikei.ac.jp (Y. Uezono).

https://doi.org/10.1016/j.biopha.2021.111800
Received 1 March 2021; Received in revised form 13 May 2021; Accepted 24 May 2021
Available online 24 June 2021

1. Introduction

Intractable pain often occurs in cancer patients, and opioid medications are commonly used to reduce such pain [1]. Opioid agonists for pain management usually target μ- (MOR), δ- (DOR) and κ-opioid receptors (KOR), and the most commonly used agents such as morphine, oxycodone, and fentanyl, mainly activate MORs [2]. Although appropriate pain-relieving treatments are available, approximately 80% of patients with advanced cancer still experience moderate to severe pain [1]. Accordingly, there is an urgent need to develop analgesics for cancer pain. The addiction and abuse of opioids is a global issue, and this opioid crisis had led to numerous deaths by opioid overdose, especially in recent times [3,4]. Novel effective treatments with fewer side-effects or methods of reducing the opioid dosage are thus needed to solve this issue [5]. The only drugs currently available to reverse opioid overdose are naloxone and naltrexone, yet treatment options remain limited.

Endothelin are peptides consisting of 21 amino acids, having isoforms such as endothelin-1 (ET-1), ET-2, and ET-3, which were first discovered as strong vascular endothelium-derived vasoconstrictors [6]. They are involved in numerous pathophysiological conditions such as pain [7]. Endothelins bind to endothelin A receptor (ETAR) and endothelin B receptor (ETBR), inducing responses that oppose each other [8,9]; ETAR induces vasoconstriction, while ETBR induces vasodilation [8,9]. Endothelins have therefore attracted attention as drug targets, especially for cardiovascular diseases [10,11]. ETAR activation stimulates sensory neurons to cause pain hypersensitivity, while ETBR has analgesic effects; [12–14] moreover, blocking endothelin receptors causes pain-related signal suppression [15–17]. Although ETBR antagonists have additionally been reported to have some analgesic effects [18], there are many reports of ETBR antagonists having no analgesic effect. Drugs targeting ETARs should ideally inhibit ETAR but not ETBR. Although bosentan, which is clinically used for pulmonary arterial hypertension [19], is known to be an ETAR and ETBR antagonist, there are no clinically available antagonists that selectively inhibit ETARs. Consequently, developing drugs targeting ETARs is warranted. In animal studies, selective ETAR antagonists enhance opioid analgesia, release endogenous opioids, and improve opioid withdrawal symptoms [20–22]; the mechanisms by which ETAR antagonists enhance the analgesic effects of opioids are unclear to date.

Additionally, one way of addressing the concerns regarding opioids is through the process of heterodimerization. By the heterodimerization of G protein coupled receptors (GPCRs), GPCRs dimerize with other GPCRs, leading to signal transduction pathways alternative to the monomeric GPCRs. The dimeric GPCR are widely studied drug targets [23–25]. ORs, the targets of morphine-induced analgesia, can heterodimerize with other GPCRs [26,27], and MOR/DOR heterodimers were demonstrated to play important roles in regulating opioid analgesia, as shown both in vitro and in vivo [28,29].

As GPCR heterodimers transmit signals differently from GPCR monomers and alter receptor-ligand signaling sensitivity [26,30], MORs can dimerize with other GPCRs and alter ligand-induced responses [28,29]. As per previous studies, GPCRs like cannabinoid CB1 receptors (CB1R) and MOR heterodimerized on cell membranes and caused functional responses that were not observed in cells expressing MOR or CB1R alone [31]. Moreover, the expression of α2A-adrenergic receptors and MOR enhanced the effects of morphine, which were not detected in cells expressing MOR alone [32]. Based on these, we hypothesized that attenuation of morphine-induced analgesic effects by ET-1 occurred through dimerized ETAR and MOR. The complete understanding of the heterodimerization mechanism remains elusive despite the recent advances in technology and further research is warranted.

We hypothesized that ETAR and MOR could dimerize and be involved in ETAR antagonist-induced opioid analgesia [16]. Therefore, this study used the novel and most ETAR-selective antagonist available, Compound-E [33], to determine whether the analgesic potentiation of opioids by ETAR antagonists is mediated through dimerized ETAR/MOR, in in vitro and in vivo models.

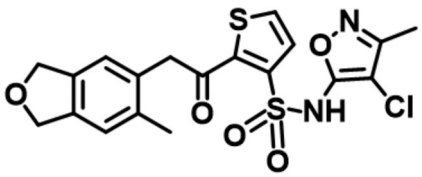

Fig. 1. Molecular structures of Compound-E.

2. Materials and methods

2.1. Constructing expression vectors

A Jump-In system compatible bidirectional expression vector carrying the hygromycin-resistant gene (pBI-CMV1-IRES-hygro-PhiC31) was constructed as follows: The internal ribosomal entry site and hygromycin-resistant gene was PCR-amplified from the pIREShyg2 vector (Takara Bio Inc., Shiga, Japan) and inserted downstream of MCS1 in pBI-CMV1 (Takara Bio Inc.). A PhiC31 sequence was PCR-amplified from pJTI Fast Dest (Invitrogen, Carlsbad, CA, USA) and inserted downstream of the SV40 polyA sequence of MCS1 in the same vector. For SNAP-MOR expression, cDNAs for the IL6 signal sequence, SNAP-tag, and coding sequence of MOR were amplified from pFN21KSPc-ORXR (FHC02116, Promega, Madison, WI, USA), pSNAPf (New England Biolabs Inc., Ipswich, MA, USA), and FL-MORhyg (Invitrogen), respectively, and ligated in tandem into MCS1 of the above vector using an infusion reaction. For Halo-ETAR and Halo-ETBR expression, HaloTag-ETAR and Halo-ETBR were PCR-amplified from pFN21A-EDNRA (Promega, FHC03517) and pFN21A-EDNRB (Promega, FHC02116), respectively, and the IL6 signal sequence was PCR-amplified from pFN21KSPc-ORXR. The PCR fragments were ligated in tandem into MCS2 of pBI-CMV1-IRES-hygro-PhiC31 using an infusion reaction. For dual expression of SNAP-MOR and Halo-ETAR, the IL6 signal-SNAP-MOR sequence was excised by *MluI*/*Not*I and inserted into MCS1 of the Halo-ETAR expression vector.

2.2. Generating stable cells

Halo-ETAR, SNAP-MOR, SNAP-MOR/Halo-ETAR and Halo-ETBR expression vectors were co-transfected with pJTI PhiC31 (Invitrogen) into HEK293 cells. The transfected cells were cultured for two weeks in Dulbecco's Modified Eagle Medium supplemented with 10% fetal calf serum, 2 mM glutamine, and 100 μg/mL hygromycin. Several hygromycin-resistant colonies were tested for protein expression by western blot (Supplementary Fig. 1) and those with suitable expression were used for subsequent experiments.

2.3. Cell culture

Cells expressing each vector were cultured in Dulbecco's Modified Eagle Medium supplemented with 10% fetal bovine serum, 1% penicillin/streptomycin, and 100 μg/mL hygromycin B solution (FUJIFILM Wako Pure Chemical Corporation, Osaka, Japan) in a humidified atmosphere containing 5% CO_2 at 37 °C. Cells between passages 3 and 10 were used for the subsequent experiments.

2.4. Drugs

The following reagents were used: forskolin (Sigma-Aldrich, St. Louis, MO, USA); ET-1, BQ-123 sodium salt, BQ-788 sodium salt (Peptide Institute, Inc., Osaka, Japan), morphine hydrochloride (Takeda Pharmaceutical Co., Ltd., Tokyo, Japan), Bosentan Monohydrate (Tokyo Chemical Industry Co., Ltd., Tokyo, Japan); and Compound-E (provided

by Eisai Co., Ltd., Tokyo, Japan, Fig. 1) [33]. ET-1 was diluted in 0.1% acetic acid. BQ-123 sodium salt, BQ-788 sodium salt, and Compound-E were diluted in DMSO, while other chemicals were diluted in H_2O.

2.5. CellKey™ assay

The CellKey™ assay, a label-free cell-based assay that detects G protein-coupled receptor activity, was used as described previously [34,35]. Briefly, cells were seeded at 7.0×10^4 (Halo-ETAR, SNAP-MOR, or Halo-ETAR/SNAP-MOR) or 5.0×10^4 (HEK293) cells/well in 96-well microplates, and incubated for 24 h. CellKey™ buffer composed of Hank's balanced salt solution (HBSS) (in mM: 1.3 $CaCl_2 \cdot 2H_2O$, 0.81 $MgSO_4$, 5.4 KCl, 0.44 KH_2PO_4, 4.2 $NaHCO_3$, 136.9 NaCl, 0.34 Na_2HPO_4, and 5.6 D-glucose) containing 20 mM HEPES and 0.1% bovine serum albumin. The medium was replaced with the assay buffer or pretreatment reagents for 30 min at 28 °C. Impedance current (dZiec) changes were measured every 10 s for 30 min [34,35]. The magnitude of changes in dZiec values were defined as ΔZiec.

2.6. cADDis cAMP assays

Cyclic adenosine monophosphate (cAMP) production in living cells was measured using the cADDis cAMP assay kit (#U0200G) (Montana Molecular, Bozeman, MT, USA). Briefly, cells were seeded at 7.0×10^4 cells/well (SNAP-MOR or Halo-ETAR/SNAP-MOR) on black-walled, clear flat-bottom 96-well plates with recombinant BacMam virus expressing the cADDis sensor and 0.6 μM sodium butyrate, and incubated for 24 h at 5% CO_2 at 37 °C. The medium was replaced with 100 μL of Krebs solution or pretreatment reagents. The 96-well plates were incubated at 28 °C for 30 min in the dark. Cell fluorescence was measured from the plate bottom using excitation/emission wavelengths of 485 and 525 nm, respectively, using the FlexStation 3 (Molecular Devices, LLC., San Jose, CA, USA). Cells were stimulated with 50 μM forskolin to increase cAMP levels. After 20 min, when the signal plateaued, cells were stimulated with the indicated drugs, and fluorescence changes in each well were measured every 26 s for 40 min. Data were transformed to the change in fluorescence over the initial fluorescence ($\Delta F/F_0$).

2.7. Pulldown of GPCR heterodimer

Halo-ETAR was precipitated using HaloTag® purification and pulldown technologies according to the manufacturer's instructions. Briefly, Magne HaloTag beads were washed thrice with washing buffer (tris-buffered saline containing 0.05% Igepal). The cells were lysed at 4 °C for 20 min in RIPA buffer (1% Nonidet P-40, 0.5% sodium deoxycholate, 0.1% SDS, 25 mM Tris-HCl pH 7.5, 137 mM NaCl, 3 mM KCl, and protease inhibitor cocktail [Complete, Roche Diagnostics, Mannheim, Germany]) [36]. Cell lysates (input) were incubated at 25 °C for 90 min with washed beads with continuous stirring. The supernatants (unbound) were incubated at room temperature for 1 h with lithium dodecyl sulfate (LDS) sample buffer with dithiothreitol (DTT). The beads were washed four times with cold RIPA buffer and incubated with Tobacco Etch Virus protease at 25 °C for 90 min. The bound proteins (bound) were eluted at room temperature for 1 h with 2 × LDS sample buffer with DTT. The bound and unbound proteins were electrophoresed and immunoblotted.

2.8. Live cell imaging

Cells cultured on μ-slide 8-well plates (ibidi, Germany) were incubated with HaloTag Alexa Fluor 488 ligand (HT-488, Promega) and SNAP surface 594 (ST-594, New England Biolabs Inc.) in HBSS(+) supplemented with 5 mM HEPES and 0.05% bovine serum albumin at 25 °C for 30 min. For live cell imaging analysis, we used a Leica SP5 confocal laser-scanning microscope equipped with an inverted microscope and two hybrid GaAs-detectors (Leica Microsystems, Wetzlar, Germany). Multipoint time-lapse images were acquired every 30 s for 30 min. The pinhole diameter was one airy unit. For multicolor total internal reflection fluorescence (TIRF) microscopy, we used a Leica AM TIRF MC custom-equipped by the manufacturer with a 100 ×, 1.46 numerical aperture oil-immersion objective, along with 405, 488, 561, and 635 nm lasers with the EM-CCD camera system (ImagEM; Hamamatsu Photonics). Time-lapse images were acquired every 1 s for 12 min. During imaging, cells were kept in HBSS with 5 mM HEPES and 0.05% bovine serum albumin at 25 °C. Images were acquired and analyzed with LAS AF (Leica Microsystems), ImageJ/Fuji (National Institutes of Health, Bethesda, Maryland, USA), or MetaMorph software (Molecular Devices).

We measured the fluorescence intensity and area of intracellular Halo-ETAR and SNAP-MOR using MetaMorph software. Intracellular fluorescent puncta were automatically selected from the binary image. The fluorescence intensity of the cell surface was defined as the background threshold.

2.9. In vivo experiments

All experiments were performed in accordance with the Ethics Committee guidelines and were approved by the Committee for Animal Experimentation of Juntendo University (approval number 310038) and complied with the "Guide for the Care and Use of Laboratory Animals" NIH publication No. 86–23, revised 2011. 8-week-old male C57BL6/J mice (20–27 g; CLEA Japan, Inc., Tokyo, Japan) were used. Food and water were available ad libitum and animals were housed in a room maintained at 22 ± 1 °C with a 12-h light-dark cycle (light on 8:00 a.m. to 8:00 p.m.). Mice were randomly divided into six groups (n = 5–8). Group 1: Compound-E vehicle (0.5 w/v% methyl cellulose (FUJIFILM Wako Pure Chemical Corporation), p.o.) and vehicle of morphine (saline, s.c.); Group 2: Compound-E (20 mg kg^{-1}, p.o.) and saline, s.c.; Group 3: 0.5 w/v% Methyl Cellulose, p.o. and morphine hydrochloride (Daiichi Sankyo Co., Ltd., Tokyo, Japan) (3 mg kg^{-1} or 10 mg kg^{-1}, s.c.); Group 4: Compound-E (20 mg kg^{-1}, p.o.) and morphine (3 mg kg^{-1} or 10 mg kg^{-1}, s.c.).

2.10. Randall-Selitto test

The analgesic responses to morphine were assessed using the Randall-Selitto electronic algesimeter (RODENT PINCHER (For Mice) BIO-RP-M (Bioseb, Vitrolles, France)). This test involves applying a uniformly increasing mechanical pressure on the animal paw. The pressure-induced pain leads to an escape reaction. Before starting the experiments, the animals acclimated to handling-related stress. They were then immobilized with the sling suits (Lomir Biomedical Inc., Montreal, Canada). The tests were performed before and 1, 1.5, 2, and 3.5 h after oral Compound-E administration. Nociceptive threshold measurements were repeated five times at approximately 5 s intervals. The five residual values were averaged to determine the threshold. Measurements were taken from the first observed behavior of vocalization, struggle, or withdrawal. A cutoff value of 600 g was used to prevent injury to the animal. The changes in withdrawal threshold from the basal value were plotted with time. The analgesic responses are presented as mean ± standard error of the mean (SEM) changes from the baseline withdrawal threshold. The analgesic responses in each mouse were converted into the area under the time-response curve (AUC0→3.5 h).

2.11. Body temperature and locomotor activities

Body (rectal) temperature was measured using a digital thermistor (DTM-900, Natsume Seisakusho Co., Ltd., Tokyo, Japan) before and after (0.5, 1, 1.5, 2, 3.5 h) oral Compound-E administration. The changes in temperature from the basal value were plotted with time.

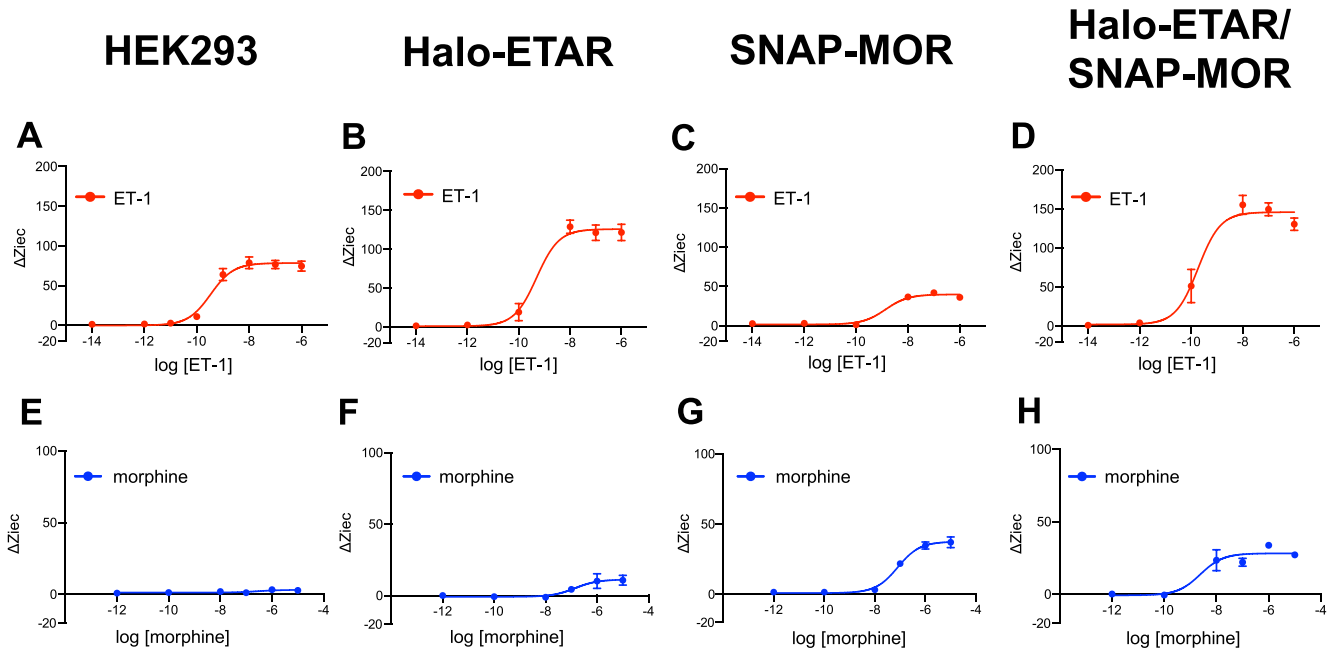

Fig. 2. Properties of endothelin-1 (ET-1) or morphine treatment in HEK293 cells expressing Halo-ETAR, SNAP-MOR and Halo-ETAR/SNAP-MOR or HEK293 cells measured using CellKey™ assay. A–D: Effects of ET-1 (10^{-14}–10^{-6} M) on the impedance activity (ΔZiec) in (A) HEK293 cells and cells expressing (B) Halo-ETAR, (C) SNAP-MOR, or (D) Halo-ETAR/SNAP-MOR. E–H: Effects of morphine (10^{-12}–10^{-5} M) on ΔZiec in (E) HEK293 cells and cells expressing (F) Halo-ETAR, (G) SNAP-MOR or (H) Halo-ETAR/SNAP-MOR. Cells were treated with ET-1 or morphine at the indicated concentrations. All points are presented as means ± SEM for 3–4 independent experiments (n = 9–12). MOR, μ-opioid receptor; ETAR, endothelin A receptor; ET-1, endothelin-1.

Locomotor activity was measured using the ACTIMO system (Shinfactory, Fukuoka, Japan). The changes in locomotor activity were plotted over time.

2.12. Statistical analysis

Data are presented as means ± SEM for at least three independent experiments. For the CellKey™ assays, one-way ANOVA followed by Dunnet tests were performed. Data from cADDis cAMP assays and in vivo experiments were analyzed with two-way ANOVA followed by the post hoc Sidak's multiple comparisons test. Western blot and live cell imaging were assessed with Student's *t*-test to compare two samples with 95% confidence. $P < 0.05$ was considered statistically significant. All analyses were performed using Prism 8 (GraphPad Software, San Diego, California, USA).

3. Results

3.1. Characterizing ETAR and MOR in HEK293 cells stably expressing Halo-ETAR, SNAP-MOR, or Halo-ETAR/SNAP-MOR

We generated HEK293 cells stably expressing Halo-ETAR, SNAP-MOR, and SNAP-MOR/Halo-ETAR (Supplementary Fig. 1). We used the CellKey™ system established in our laboratory [34] to measure whole-cell ETAR and/or MOR activity. ET-1 increased cellular impedance in all cells in a concentration-dependent manner (Fig. 2A–D). Log half maximal effective concentration ($logEC_{50}$) values of ET-1 in the HEK293 cells and HEK293 cells stably expressing Halo-ETAR, SNAP-MOR and Halo-ETAR/SNAP-MOR were −9.67 ± 0.12, −9.30 ± 0.23, −8.86 ± 0.24 and-9.73 ± 0.17, respectively (n = 9–12 each). Since ETAR and ETBR are endogenously expressed in host HEK293 cells, we used the novel ETAR selective antagonist Compound-E and ETBR-selective antagonist BQ-788, respectively, to compare their responses. Compound-E suppressed the ET-1 response in HEK293 and SNAP-MOR cells (Supplementary Fig. 2A and C) but did not completely suppress in Halo-ETAR or Halo-ETAR/SNAP-MOR cells, possibly due to ETAR overexpression (Supplementary Fig. 2B and D). BQ-788 almost

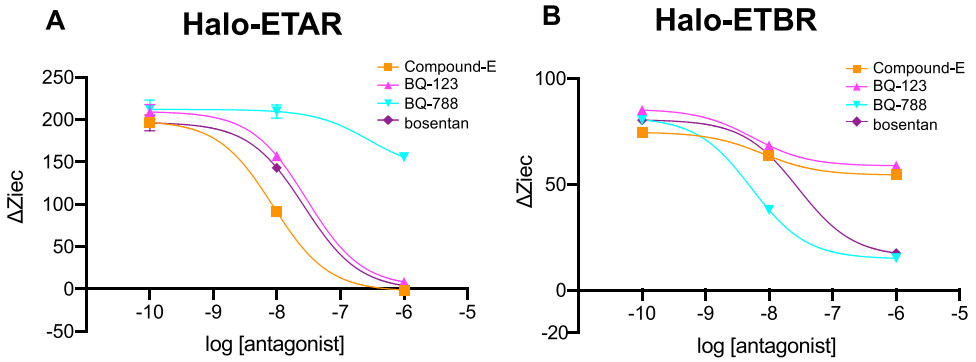

Fig. 3. Selectivity of ETR antagonists in HEK293 cells stably expressing Halo-ETAR or Halo-ETBR measured using CellKey™ assay. A, B: Effects of Compound-E, BQ-123, BQ-788, or bosentan (10^{-10}–10^{-6} M) on the impedance activity (ΔZiec) in HEK293 cells expressing (A) Halo-ETAR, or (B) Halo-ETBR. Cells were treated with 10^{-8} M ET-1. Concentration-response curves of each antagonist were described by calculating ΔZiec relative to the data obtained at 10^{-10} M Compound-E treatment. All points are presented as means ± SEM for 3 independent experiments (n = 9). ETAR, endothelin A receptor; ETBR, endothelin B receptor.

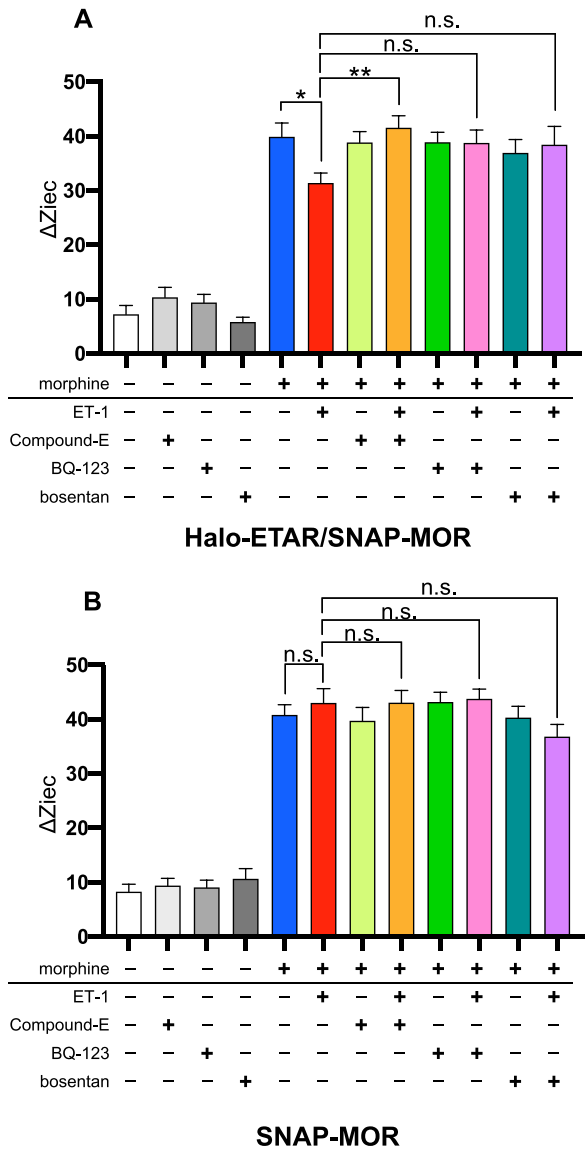

Fig. 4. Evaluation of μ-opioid receptor (MOR) activity by 10^{-6} M morphine and ET-1 with or without endothelin A receptor (ETAR) antagonists using CellKey™ assay. A, B: Effects of Compound-E, BQ-123 and bosentan on morphine-induced impedance activity (ΔZiec) with or without 10^{-8} M endothelin-1 (ET-1) and/or 10^{-8} M ETR antagonists in HEK293 cells expressing (A) Halo-ETAR/SNAP-MOR and (B) SNAP-MOR. Cells were pretreated with vehicle, ET-1 (10^{-8} M) or ETR antagonists (10^{-8} M). All data are presented as means ± standard error of the mean (SEM) of three independent experiments (n = 9)*P < 0.05, **P < 0.01, in comparison to the ET-1 group (one-way ANOVA followed by the post hoc Dunnet's multiple comparisons test). MOR, μ-opioid receptor; ETAR, endothelin A receptor; ET-1, endothelin-1; n.s., Not significant.

suppressed ET-1-induced responses in HEK293 and SNAP-MOR cells (Supplementary Fig. 2A and C), and slightly suppressed in Halo-ETAR and Halo-ETAR/SNAP-MOR cells (Supplementary Fig. 2B and D). Morphine only increased cellular impedance in cells exogenously expressing SNAP-MOR (SNAP-MOR and Halo-ETAR/SNAP-MOR) in a concentration-dependent manner (Fig. 2G and H). However, morphine did not change impedance in HEK293 and Halo-ETAR cells (Fig. 2E and F). LogEC$_{50}$ values of morphine in HEK293 cells stably expressing SNAP-MOR and Halo-ETAR/SNAP-MOR were −7.09 ± 0.12 and −8.62 ± 0.38, respectively (n = 9–12 each).

3.2. Selectivity of ETR antagonists in HEK293 cells stably expressing Halo-ETAR or Halo-ETBR

We generated HEK293 cells stably expressing Halo-ETAR, and Halo-ETBR. We used the CellKey™ system established in our laboratory [34] to check the selectivity of each ETR antagonist. We used the novel ETAR selective antagonist Compound-E, conventional ETAR selective antagonist BQ-123 and ETBR-selective antagonist BQ-788, respectively, to compare their responses. ETR antagonists decreased cellular impedance in each cell in a concentration-dependent manner (Fig. 3A and B). Log half maximal inhibitory concentration (log IC$_{50}$) values of Compound-E, BQ-123, BQ-788, and bosentan in HEK293 cells stably expressing Halo-ETAR respectively were −8.06 ± 0.04, −7.53 ± 0.09, −6.55 ± 2.71 and −7.57 ± 0.09 (n = 3 each). Log IC$_{50}$ values of them in HEK293 cells stably expressing Halo-ETBR were −8.10 ± 0.26, −8.25 ± 0.30, −8.28 ± 0.14 and − 7.54 ± 0.11, respectively. ETAR antagonists, Compound-E and BQ-123, suppressed the ET-1 response in Halo-ETAR cells. Furthermore, Compound-E shifted the dose-response curve of ET-1 to the left. (Fig. 3A). Although, Compound-E and BQ-123 did not completely suppress in Halo-ETBR cells (Fig. 3B), BQ-788 suppressed ET-1-induced responses in Halo-ETBR cells (Fig. 3B), and slightly suppressed in Halo-ETAR cells (Fig. 3A).

3.3. Evaluating augmented MOR activity by ETAR antagonists

Since ET-1 expression increases under pain [37–40], we pretreated cells with ET-1 to mimic pain in vitro and determined changes in morphine activity with different ETAR antagonists. We used Compound-E as a novel and selective ETAR antagonist, BQ-123 as a typical ETAR antagonist [41], and bosentan as another ETAR/ETBR antagonist [19]. ET-1 pretreatment in Halo-ETAR/SNAP-MOR cells overexpressing ETAR attenuated morphine-induced responses [F(8, 194) = 10.04, p < 0.05] (Fig. 4A). However, ET-1 pretreatment did not change morphine-induced responses in SNAP-MOR cells expressing lower ETAR levels [F(8, 216) = 30.94, p > 0.05] (Fig. 4B). The antagonists did not affect the MOR-induced responses in Halo-ETAR/SNAP-MOR cells [F(8, 194) = 10.04, p > 0.05] and SNAP-MOR cells [F(8, 216) = 30.94, p > 0.05]. Compound-E significantly restored the ET-1-induced attenuation of morphine responses [F(8, 194) = 10.04, p < 0.01] (Fig. 4A). Furthermore, Compound-E increased these effects in a concentration-dependent manner (Supplementary Fig. 3). BQ-123 and bosentan did not restore ET-1 induced attenuation of morphine responses at low concentrations, however, they restored this attenuation at high concentrations (Supplementary Fig. 3).

We performed a cAMP assay with cADDis sensors to confirm that only GPCR signals contribute to the analgesic action [42] as the cAMP pathway is conducted through the Gi-mediated pathway [34]. ET-1 pretreatment attenuated morphine responses in Halo-ETAR/SNAP-MOR cells [F(5, 132) = 16.11, P < 0.0001, F(5, 132) = 7.535, P < 0.0001 and F(5, 96) = 14.78, P < 0.0001] (Fig. 5A–C; left), but not in SNAP-MOR cells [F(5, 96) = 0.2696, P > 0.05, F(5, 96) = 0.02724, P > 0.05 and F(5, 96) = 0.8129, P < 0.05] (Fig. 5A–C; right). Compound-E [F(5, 132) = 3.546, P < 0.01], but not BQ-123 [F(5, 132) = 0.7532, P > 0.05] and bosentan [F(5, 96) = 1.246, P > 0.05], improved ET-1-induced attenuation of morphine responses (Fig. 5A–C; left).

3.4. Co-immunoprecipitation of Halo-ETAR and SNAP-MOR

We performed a co-immunoprecipitation of ETAR and MOR in HEK293 cells expressing Halo-ETAR, Halo-ETAR/SNAP-MOR, or SNAP-MOR. Halo-ETAR was detected in the input and unbound of Halo-ETAR cells and Halo-ETAR/SNAP-MOR cells. Furthermore, ETARs were detected in Halo-ETAR and Halo-ETAR/SNAP-MOR cell precipitates (Fig. 6A). In Halo-ETAR/SNAP-MOR cell precipitates, SNAP-MORs were also detected (Fig. 6B). Quantitative analysis of co-precipitated SNAP-

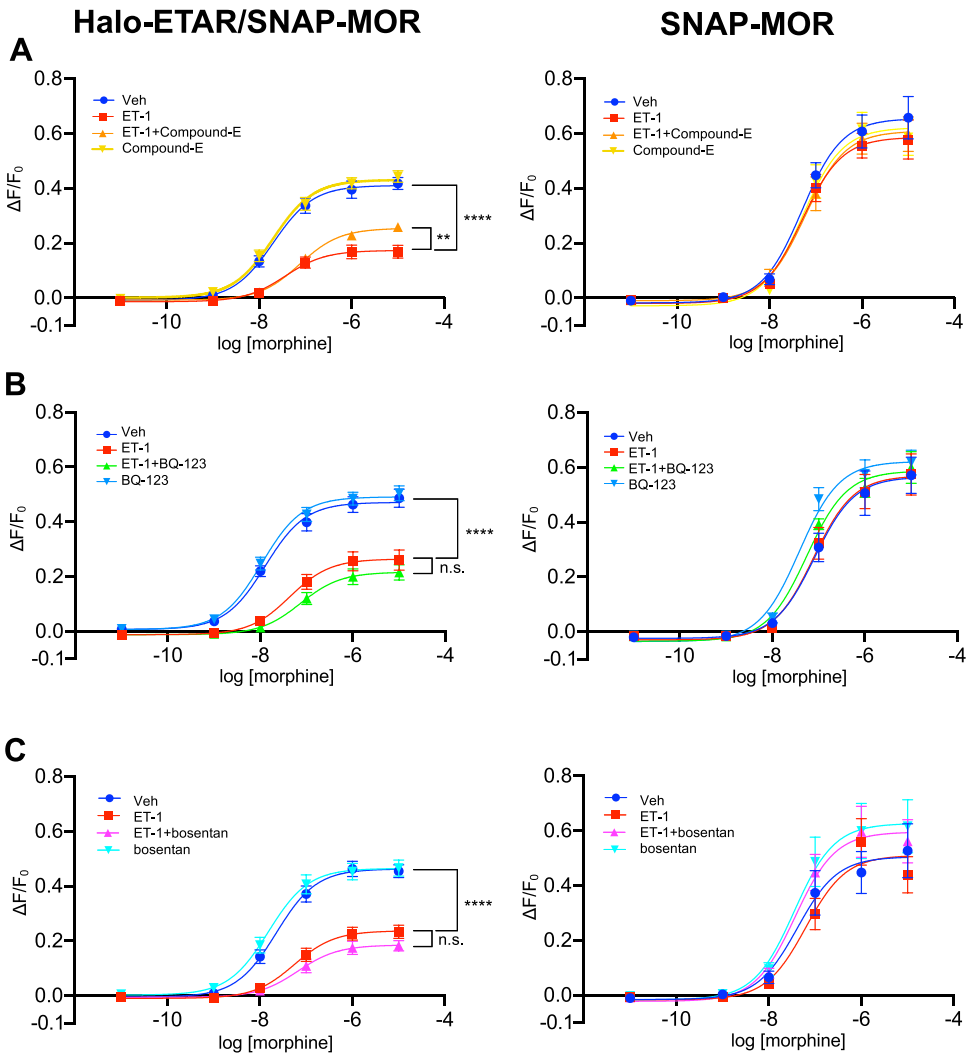

Fig. 5. Evaluation of μ-opioid receptor (MOR) activity with endothelin-1 (ET-1) and/or endothelin A receptor (ETAR) antagonists using cAMP assay. A: Concentration-response curves for morphine-induced cAMP levels with or without 10^{-8} M ET-1 and/or Compound-E in HEK293 cells expressing (Left) Halo-ETAR/SNAP-MOR and (Right) SNAP-MOR. B: Concentration-response curves of morphine-induced cAMP levels with or without 10^{-8} M ET-1 and/or BQ-123 in cells expressing (Left) Halo-ETAR/SNAP-MOR and (Right) SNAP-MOR. C: Concentration-response curves of morphine-induced cAMP levels with or without 10^{-8} M ET-1 and/or bosentan in cells expressing (Left) Halo-ETAR/SNAP-MOR and (Right) SNAP-MOR. Cells were pretreated with ET-1 (10^{-8} M), with or without each ETAR antagonist (10^{-8} M). All data are presented as means ± SEM of 3–4 independent experiments (n = 9–12); **P < 0.01, ****P < 0.0001, in comparison to ET-1 group (two-way ANOVA followed by the post hoc Sidak's multiple comparisons test). MOR, μ-opioid receptor; ETAR, endothelin A receptor; Veh, vehicle; ET-1, endothelin-1; n.s., Not significant.

MOR revealed that SNAP-MOR in Halo-ETAR/SNAP-MOR cells clearly increased compared to SNAP-MOR cells (t = 3.231, P < 0.05) (Fig. 6C).

3.5. Co-localization of ETAR and MOR upon TIRF microscopy in Halo-ETAR/SNAP-MOR cells

TIRF microscopy showed colocalization of ETAR and MOR in Halo-ETAR/SNAP-MOR cells (Fig. 7A), suggesting a close interaction between ETAR and MOR on cell membranes. The 2-min time-lapse showed that Halo-ETAR and SNAP-MOR were co-transported into the cytosol (Supplementary Fig. 4).

3.6. ETAR/MOR dimer interactions

Halo-ETAR/SNAP-MOR cells were stimulated with ET-1 (10^{-7} M) and the punctae that translocated into the cell were visually quantified (Fig. 7B; left). ET-1 stimulation significantly increased the number of puncta in the overlay (yellow) (t = 4.714, P < 0.0001) (Fig. 7B; right). The 30-min time-lapse showed that the number of puncta of the overlay increased (Supplementary Fig. 4). However, the number of puncta stained with HT-488 or ST-549 alone did not change before and after stimulation (t = 1.155, P > 0.05 and t = 0.5142, P > 0.05) (Fig. 7B; right). Monomeric or homodimeric ETARs or MORs did not cause ET-1-induced endocytosis; however, the heterodimerized ETAR/MORs caused ET-1-induced endocytosis (Fig. 7B; right).

We further stimulated Halo-ETAR/SNAP-MOR cells with ET-1 (10^{-7} M) and automatically measured the changes in puncta (Fig. 7C; left). ET-1 stimulation increased the number of puncta (t = 5.480, P < 0.001) (Fig. 7C; middle). The area of the puncta in cells remained unchanged (t = 0.4674, P > 0.05) (Fig. 7C; right), indicating early-stage endocytosis without changing the internalized receptor size or shape. There was no change in fluorescence intensity for Halo-ETAR or SNAP-MOR alone before and after ET-1 stimulation, suggesting that SNAP-MOR likely formed ETAR/MOR dimers rather than existing alone (Supplementary Fig. 5).

3.7. Effect of Compound-E on morphine-induced pain sensitivity in mice

We evaluated the effects of morphine on the analgesic action using the Randall-Selitto test. Mice were injected with morphine (3 or 10 mg kg^{-1}), the withdrawal threshold was measured, and data were normalized to those at 0 h. In the control and Compound-E-treated mice, the withdrawal threshold remained unchanged over 3.5 h [F(4, 190) = 0.3262, P > 0.05] (Fig. 8A), indicating that Compound-E treatment alone did not affect the withdrawal threshold. Morphine elicited analgesia in mice, which persisted for 3 h [F(4, 270) = 12.21, P < 0.0001] (Fig. 8A). The analgesic action increased, peaked at 30 min, and then gradually decreased by 43.5% (3 mg kg^{-1}) and 38.1% (10 mg kg^{-1} morphine) (Fig. 8A). Compound-E pretreatment significantly increased the morphine-induced withdrawal threshold as well as the analgesic effects of morphine [F(4, 350) = 5.394, P < 0.001 and F(4, 350) = 6.898, P < 0.0001] (3 or 10 mg kg^{-1}), which persisted for 3 h (Fig. 8A).

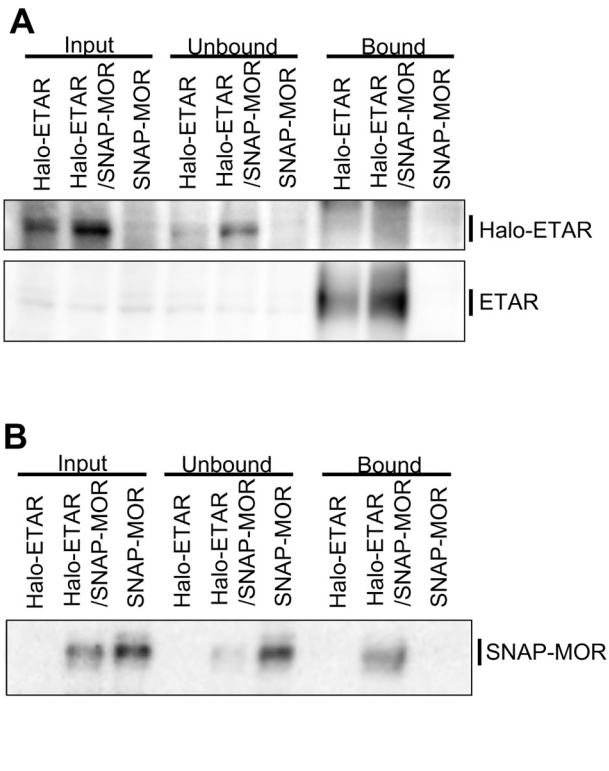

Fig. 6. Immunoprecipitation of cell lysates expressing Halo-ETAR, SNAP-MOR, or Halo-ETAR/SNAP-MOR. Cell lysates were precipitated with Magnet-based HaloTag beads. The input control (Input), supernatants (Unbound), and precipitates (Bound) were electrophoresed and immunoblotted for antibodies against (A) Halo-ETAR and ETAR and (B) SNAP-tag. A: Halo-ETAR was detected in the input and unbound of Halo-ETAR cells and Halo-ETAR/SNAP-MOR cells. ETAR was detected in the precipitates of Halo-ETAR cells and Halo-ETAR/SNAP-MOR cells. B: SNAP-MOR was detected in the precipitate of Halo-ETAR/SNAP-MOR cells. C: Quantitative analysis of co-precipitated SNAP-MOR. The precipitated SNAP-MOR signals were normalized to input control. Statistical significance was tested by unpaired *t*-test. *$P < 0.05$. Data are mean ± SEM based on three independent experiments ($n = 3$). MOR, μ-opioid receptor; ETAR, endothelin A receptor.

The analgesic effect of morphine peaked (3 mg kg^{-1}; 198.27 ± 7.84 g, 10 mg kg^{-1}; 249.38 ± 10.35 g) at 30 min after administration; it gradually decreased by 26.4% and 36.6% after administration (3 or 10 mg kg^{-1}) at 3 h, respectively (Fig. 8A). The AUC of the withdrawal threshold was 32.16 ± 7.28 g in the control group and 26.35 ± 8.60 g in the Compound-E-treated group. The AUC was 105.52 ± 8.33 g and 158.93 ± 16.19 g in morphine (3 or 10 mg kg^{-1})-treated mice, respectively. The AUC for Compound-E + morphine (3 or 10 mg kg^{-1})-treated mice was 208.55 ± 16.88 g and 313.76 ± 19.32 g, respectively (Fig. 8B).

3.8. Effect of Compound-E on morphine-induced changes in body temperature in mice

The baseline body temperature before drug treatment was 37.79 ± 0.05 ℃. In the control and Compound-E-treated groups, body temperature did not change over 3.5 h [$F(5, 48) = 0.7682$, $P > 0.05$] (Fig. 9A), demonstrating that Compound-E treatment alone did not affect body temperature. Morphine (3 mg kg^{-1}, s.c.) induced slight hypothermia, lasting for 1.5 h [$F(5, 72) = 2.092$, $P = 0.0762$] (Fig. 9A). Morphine (10 mg kg^{-1}) also induced significant hypothermia, lasting for 3 h [$F(5, 72) = 8.391$, $P < 0.0001$], and Compound-E + morphine significantly improved the morphine-induced hypothermia, lasting for over 3 h [$F(5, 96) = 3.704$, $P < 0.01$] (Fig. 9A).

3.9. Effect of Compound-E on morphine-induced changes in locomotor activity

In the control and Compound-E group, locomotor activity remained unchanged over 3.5 h. Morphine (3 or 10 mg kg^{-1}, s.c.) induced concentration-dependent hyperactivity in mice, lasting for over 3 h. Morphine (10 mg kg^{-1}) induced significant hyperactivity in mice, lasting over 3 h. Compound-E pretreatment followed by morphine augmented the increase in morphine-induced hyperactivity (Fig. 9B).

4. Discussion

In our in vitro study, ET-1 attenuated the analgesic effect of morphine under pain conditions. Furthermore, the novel and highly ETAR-selective antagonist, Compound-E, restored the ET-1-induced attenuating effects on morphine. The attenuating effect of ET-1 on MOR activity was possibly caused by ETAR/MOR heterodimerization. Our in vivo study demonstrated that Compound-E and morphine co-administration enhanced the analgesic effect of morphine. These results suggest that the morphine-induced analgesic effects attenuated by ET-1 were restored by Compound-E through inhibition of the activity of dimerized ETAR/MOR.

The analgesic effects of morphine are predominantly mediated by Gi protein-mediated pathways [43,44]. The CellKey™ assay system measures most membrane protein responses, including GPCRs, in real-time [34]. These changes reflect ligand-induced receptor reactions in whole-cell events, but it may be difficult to identify whether the responses are from the G protein- or the β arrestin-mediated pathway. To further clarify the effects, we employed the cADDis cAMP assay system that solely detects responses by G protein-mediated pathways. We confirmed that morphine attenuation by ET-1 indeed occurred by suppression of the G protein-mediated signaling pathway. Compound-E may affect morphine-induced β-arrestin signaling and Gi signaling separately. Therefore, if it selectively promotes Gi signaling rather than β-arrestin signaling, Compound-E may be a better drug to promote analgesia alone; this requires further investigation.

ET-1 and ETAR expression levels increase during pain [37–40]. As ETAR expression in ETAR/MOR cells were higher than that in MOR-expressing HEK293 cells endogenously expressing endothelin receptors, we speculated that pain was reproduced by pretreatment with ET-1 in ETAR-overexpressed ETAR/MOR cells. We did not observe this response in SNAP-MOR-expressing cells where endogenous ETAR expression was lower, suggesting that ET-1 attenuated the effects of morphine in cells where high levels of ETAR were expressed. Currently, there are no reports on the role of ET-1 in the analgesic tolerance of morphine, nor on the involvement of dimerized ETAR/MORs in pain.

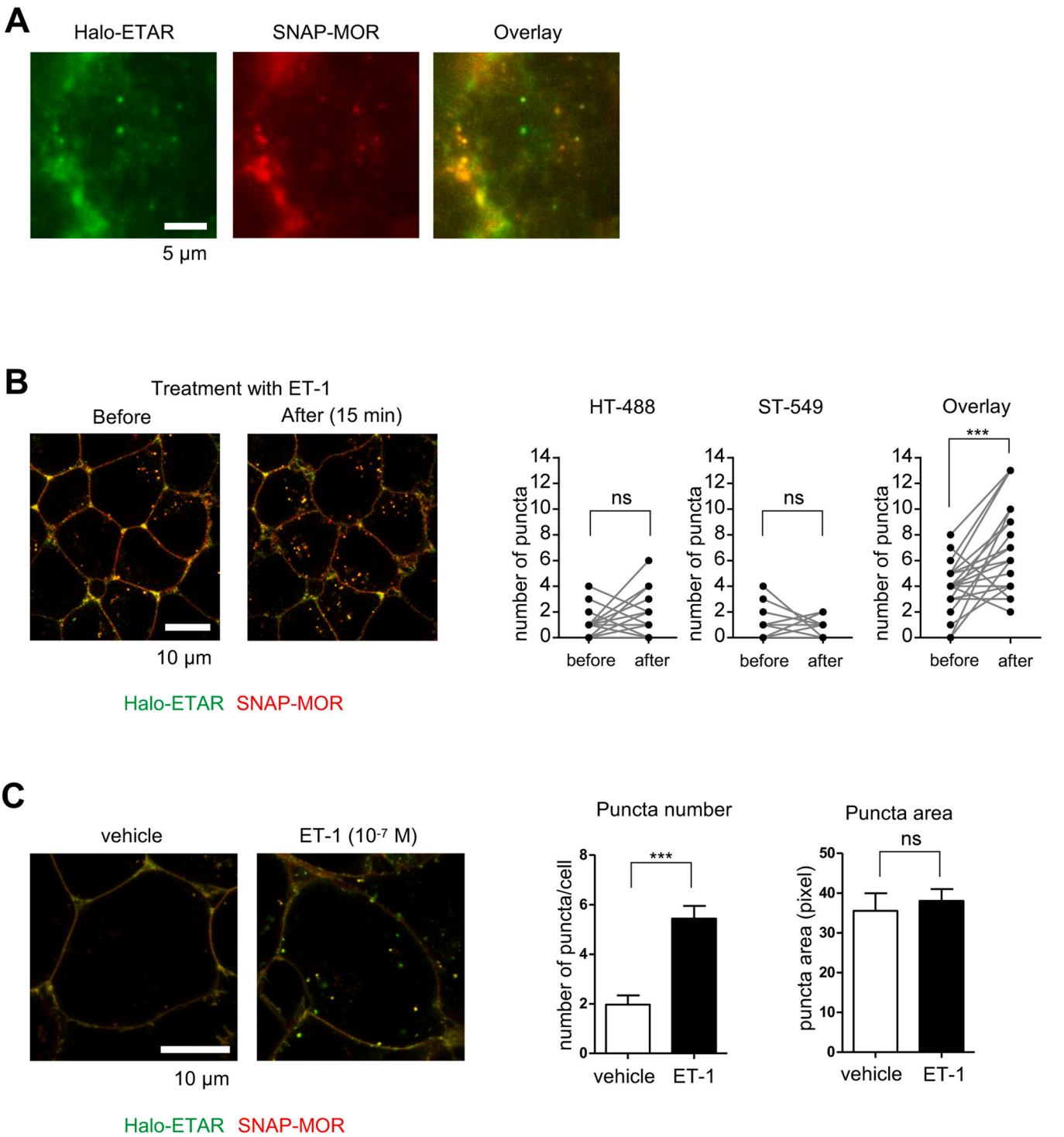

Fig. 7. Live cell imaging of cells transfected with Halo-ETAR and SNAP-MOR. Live cells expressing Halo-ETAR and SNAP-MOR were stained with fluorescent-labeled Halotag and SNAP-tag substrates at 25 °C for 30 min. ETAR was labeled with HaloTag Alexa Fluor 488 ligand (Green, HT-488), and MOR was labeled with SNAP surface 594 (Red, ST-549). A: Total internal reflection fluorescence microscopic images of Halo-ETAR/SNAP-MOR cells. Scale bar; 5 μm. Penetration depth; 90 nm. B: Fluorescence images of Halo-ETAR/SNAP-MOR cells treated with 10^{-7} M ET-1. Cells were stained with HT-488 (green) and ST-549 (red) ligand and treated with 10^{-7} M ET-1 for 0–15 min at 25 °C (Left). Puncta were labeled with HT-488 only, ST-594 only, or HT-488 and ST-594 (Right). Analyses were performed with Student's *t*-test for matched pairs with 95% confidence. n = 24 cells in six photographs. C: Fluorescence images of Halo-ETAR/SNAP-MOR cells treated with 10^{-7} M ET-1 or vehicle. Cells were stained with HT-488 (green) and ST-594 (red) ligand for 30 min at 25 °C and were treated with 10^{-7} M ET-1 or vehicle for 15 min at 25 °C (Left). The intracellular HT-ETAR puncta, which has a higher fluorescence intensity than the cell surface, was automatically selected. The number (middle) and area (right) of puncta were measured by MetaMorph (software). Analyses were performed with Student's *t*-test for comparing two samples with 95% confidence. Quantitative summary data were expressed as means ± SEM. n = 6 regions including 45 (vehicle) or 57 (ET-1) cells. MOR, μ-opioid receptor; ETAR, endothelin A receptor; ET-1, endothelin-1. (For interpretation of the references to colour in this figure, the reader is referred to the web version of this article)

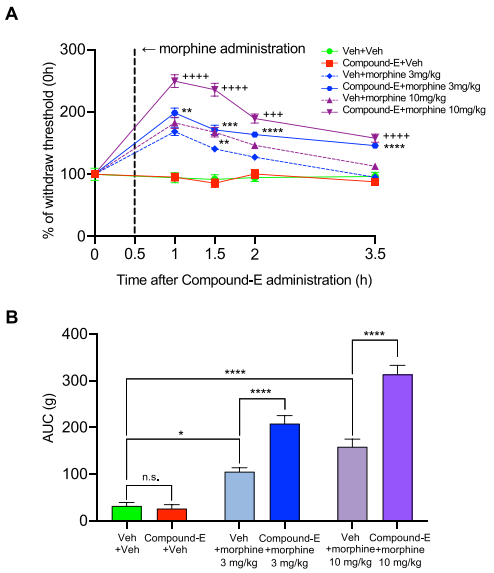

Fig. 8. Effect of Compound-E on morphine-induced pain sensitivity. Effects of Compound-E pretreatment on morphine (3 and 10 mg kg^{-1}, s.c.)-induced analgesic responses. The withdrawal threshold of each data was normalized by that of the data at 0 h (A). Effects of Compound-E pretreatment were depicted by $AUC_{0\rightarrow3.5\ h}$ (B). A: Values are mean ± SEM and n = 5–9 per group; **p < 0.01, ***p < 0.001, ****p < 0.0001 in comparison to vehicle + morphine 3 mg kg^{-1} group, +++p < 0.001, ++++p < 0.0001 in comparison to vehicle + morphine 10 mg kg^{-1} group (two-way ANOVA followed by the post hoc Sidak's multiple comparisons test). B: Values are mean ± SEM and n = 5–9 per group; *p < 0.05, ****p < 0.0001 (one-way ANOVA followed by the post hoc Tukey's multiple comparisons test). Veh: Vehicle; n.s., Not significant.

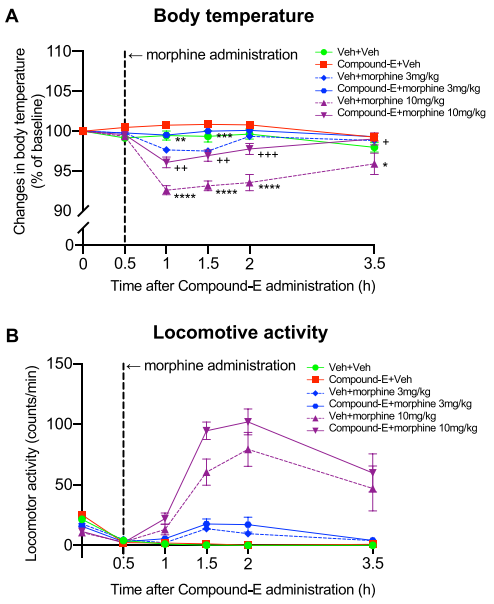

Fig. 9. Effects of Compound-E on the changes of morphine-induced body temperature and locomotor activity in mice. A: Effects of Compound-E on the morphine (3 and 10 mg kg^{-1}, s.c.)-induced changes in body temperature. The body temperature of each data was normalized by that of the data at 0 h. B: Effects of Compound-E on morphine (3 and 10 mg kg^{-1}, s.c.)-induced changes in locomotor activity. A: Values are mean ± SEM and n = 5–9 per group; **p < 0.01, ***p < 0.001 in comparison to vehicle + morphine 3 mg kg^{-1} group, +p < 0.05, ++p < 0.01, +++p < 0.001 in comparison to vehicle + morphine 10 mg kg^{-1} group (two-way ANOVA followed by the post hoc Sidak's multiple comparisons test). B: n = 1–6 per group. Veh, vehicle.

Live cell imaging also showed that overlays of ETAR and MOR puncta were increased by ET-1 stimulation. This indicates that once ETAR/MOR is dimerized and internalized, morphine becomes less effective due to less MORs on the cell membrane. Our results interestingly suggest that the presence of ET-1 and the ETAR/MOR heterodimer contribute to the analgesic tolerance of morphine.

We showed that Compound-E had superior activity on the ET-1-induced attenuating effect of morphine among the other endothelin receptor antagonists assessed. In the cAMP assay, only the highly selective ETAR antagonist significantly restored the ET-1-mediated attenuation [33]. Together, Compound-E may have a higher ameliorative effect than the existing ETAR antagonists on enhancing the analgesic effect by MOR. ETAR and MOR have been reported to co-localize in the spinal cord, spinal dorsal root ganglia, and peripheral nerves. Therefore, we assume that a functional interaction between Compound-E and morphine occurs in the nervous system. In addition, animal studies showed the enhanced locomotor activity due to the release of dopamine. Therefore, we assume that Compound-E crosses the blood brain barrier and enters the central nervous system.

In vivo, we found that Compound-E increased the intensity and duration of the analgesic effects of morphine. Another ETAR selective antagonist, BQ-123, can increase the intensity and duration of morphine-induced analgesia in the tail-flick test [20]. Based on this, the analgesic potentiation by BQ-123 was possibly not a direct effect on MORs [20], suggesting that the analgesic potentiation of MORs by ETAR antagonists may involve ETAR, and possibly the dimerization of ETAR/MOR. Further investigations are warranted to determine the involvement of dimerized ETAR/MOR on the ET-1-induced analgesic attenuation. In addition, other ETAR antagonists, BQ123 and BMS182874, prevent morphine tolerance and reversed tolerance [45]; it is possible that Compound-E may also have these effects. We need to investigate the therapeutic effects of Compound-E by using morphine-tolerant mice or rats in a future study.

Opioid agonists bind to MOR, DOR, and KOR. MORs are highly distributed in the brain and mediates most of the analgesic effects. They are also located in other organs and mediates major side-effects such as respiratory depression, euphoria, sedation, and dependence. DORs are predominantly distributed in the extrapyramidal tract and have weak analgesic effects. They are involved in emotion, causing neurotransmitter inhibition and dependence. KORs are distributed in the hypothalamus and spinal cord. They are responsible for analgesic effects at the spinal cord level, and are also involved in sedation and discomfort, not but dependence. Furthermore, the effects of each receptor on changes in body temperature differ [46]; activation of MOR induces hyperthermia, whereas activation of DOR and KOR induce hypothermia [47]. In our study, a relatively low-dose morphine (3 mg kg^{-1}) slightly decreased the body temperature in mice due to the mixed agonistic effects of each receptor. On the other hand, a high-dose of morphine (10 mg kg^{-1}) caused hypothermia. Although morphine mainly activates MOR, it also acts on DORs and KORs when administered at a large concentration, which may decrease the body temperature due to the DOR and KOR-dominant effect. Co-administration of morphine and Compound-E alleviates hypothermia; therefore, Compound-E likely enhances the action of MORs that are involved in hyperthermia to eventually restore high-dose morphine-induced hypothermia by activating MOR but not DOR and/or KOR. Although the existence of dimerized ETAR/MOR in vivo is still uncertain, the changes in body temperature by Compound-E and morphine suggest that ETARs and MORs might heterodimerize in vivo, and that Compound-E effectively augments the effects of MOR via heterodimerized ETAR/MOR.

Morphine suppresses inhibitory gamma-amino butyric acid interneuron activity via MOR activation, which activates the mesolimbic dopaminergic nervous system. This activation increases locomotor activity in mice due to the release of dopamine [48]. Simultaneous administration of morphine and Compound-E may potentiate the effects of MOR, which activates the release of dopamine to increase locomotor

activity. The enhanced locomotor activity by Compound-E and morphine co-administration observed in this study thus suggests that ETARs and MORs might be associated in vivo, and that Compound-E may augment the effects via activation of heterodimerized ETAR/MOR.

Opioids are known to cause side effects such as nausea, vomiting, constipation, drowsiness, delirium, and respiratory depression by central and peripheral opioid action [49]. Nausea and vomiting can cause a decrease in medication adherence, so preventive administration of antiemetic drugs is often used. Furthermore, the use of opioids requires measures against constipation to maintain the quality of life of patients. We found that Compound-E potentiated the effects of morphine by specifically reducing the body temperature and increasing in locomotor behavior; however, we did not examine the effects of Compound-E on the other side-effects of morphine in this study. It has been reported that the combination of other ETAR antagonists with morphine does not increase constipation [50]. In general, the data on the extent or mechanism of ETAR inhibition on the side-effects of opioids is so far, limited. Careful assessment of these effects is warranted in future studies.

5. Conclusions

Our study showed that the ET-1 that is attenuated by morphine's effects, may be through the formation of ETAR/MOR heterodimer, and that Compound-E could be a clinically important candidate for drug development. However, the clinical development and indications of Compound-E have not yet been determined. Although further study is required, one clinical application of Compound-E could be in analgesic treatment, in conjunction with opioid analgesics. Opioid administration in combination with ETAR antagonists may reduce the amount of opioid required for analgesia, and furthermore, may provide appropriate pain management in patients with an opioid addiction. In conclusion, Compound-E, a novel ETAR antagonist, may have therapeutic effects on morphine tolerance under pain. Further studies are warranted to investigate the usefulness of Compound-E as a therapeutic drug.

Author contributions

Y Kuroda, M Nonaka and Y Uezono performed entire experiments and wrote the paper. Y Uezono designed and supervised the experiments. Y Kamikubo and H Sakairi carried out the immunoprecipitation and live cell imaging of ETAR and MOR. H Ogawa, T Murayama, and N Kurebayashi constructed expression vectors and generated stable cells. K Miyano, A Komatsu provided technical and material support. T Dodo and K Nakono-Ito provided Compound-E and critically reviewed the manuscript. K Yamaguchi, T Sakurai, M Iseki, and M Hayashida contributed to data interpretation and critically reviewed the manuscript.

Acknowledgments

The authors would like to thank Seiichi Kotoda, Bio Research Center Co. Ltd., Nagoya, Japan for technical assistance with the experiments. This research was partially supported by Platform Project for Supporting Drug Discovery and Life Science Research (Basis for Supporting Innovative Drug Discovery and Life Science Research (BINDS)) from the Japan Agency for Medical Research and Development (grant Number JP20am0101080). This study was funded in part by Eisai Co., Ltd. We would like to thank Editage (www.editage.site) for English language editing.

Appendix A. Supporting information

Supplementary data associated with this article can be found in the online version at doi:10.1016/j.biopha.2021.111800.

References

[1] M.H. van den Beuken-van Everdingen, J.M. de Rijke, A.G. Kessels, H.C. Schouten, M. van Kleef, J. Patijn, Prevalence of pain in patients with cancer: a systematic review of the past 40 years, Ann. Oncol. 18 (9) (2007) 1437–1449.
[2] G.W. Hanks, F. Conno, N. Cherny, M. Hanna, E. Kalso, H.J. McQuay, S. Mercadante, J. Meynadier, P. Poulain, C. Ripamonti, L. Radbruch, J.R. Casas, J. Sawe, R.G. Twycross, V. Ventafridda, Expert Working Group of the Research Network of the European Association for Palliative Care, Morphine and alternative opioids in cancer pain: the EAPC recommendations, Br. J. Cancer 84 (5) (2001) 587–593.
[3] R.J. Blendon, J.M. Benson, The public and the opioid-abuse epidemic, New Engl. J. Med. 378 (5) (2018) 407–411.
[4] N.D. Volkow, F.S. Collins, The role of science in addressing the opioid crisis, New Engl. J. Med. 377 (4) (2017) 391–394.
[5] N.P. Coussens, G.S. Sittampalam, S.G. Jonson, M.D. Hall, H.E. Gorby, A.P. Tamiz, O.B. McManus, C.C. Felder, K. Rasmussen, The opioid crisis and the future of addiction and pain therapeutics, J. Pharm. Exp. Ther. 371 (2) (2019) 396–408.
[6] M. Yanagisawa, H. Kurihara, S. Kimura, Y. Tomobe, M. Kobayashi, Y. Mitsui, Y. Yazaki, K. Goto, T. Masaki, A novel potent vasoconstrictor peptide produced by vascular endothelial cells, Nature 332 (6163) (1988) 411–415.
[7] T.P. Smith, T. Haymond, S.N. Smith, S.M. Sweitzer, Evidence for the endothelin system as an emerging therapeutic target for the treatment of chronic pain, J. Pain Res. 7 (2014) 531–545.
[8] J.J. Maguire, R.E. Kuc, G. O'Reilly, A.P. Davenport, Vasoconstrictor endothelin receptors characterized in human renal artery and vein in vitro, Br. J. Pharm. 113 (1) (1994) 49–54.
[9] C.F. Plato, D.M. Pollock, J.L. Garvin, Endothelin inhibits thick ascending limb chloride flux via ET(B) receptor-mediated NO release, Am. J. Physiol. Ren. Physiol. 279 (2) (2000) F326–F333.
[10] M. Barton, A. Sorokin, Endothelin and the glomerulus in chronic kidney disease, Semin. Nephrol. 35 (2) (2015) 156–167.
[11] N. Vignon-Zellweger, S. Heiden, T. Miyauchi, N. Emoto, Endothelin and endothelin receptors in the renal and cardiovascular systems, Life Sci. 91 (13–14) (2012) 490–500.
[12] G.D. Nicol, ET–phone the pain clinic, Trends Neurosci. 27 (4) (2004) 177–180, discussion 180.
[13] C.S. Houck, A. Khodorova, A.M. Reale, G.R. Strichartz, G. Davar, Sensory fibers resistant to the actions of tetrodotoxin mediate nocifensive responses to local administration of endothelin-1 in rats, Pain 110 (3) (2004) 719–726.
[14] Y. Tang, H. Peng, Q. Liao, L. Gan, R. Zhang, L. Huang, Z. Ding, H. Yang, X. Yan, Y. Gu, X. Zang, D. Huang, S. Cao, Study of breakthrough cancer pain in an animal model induced by endothelin-1, Neurosci. Lett. 617 (2016) 108–115.
[15] C.M. Kopruszinski, R.C. Dos Reis, E. Gambeta, A. Acco, G.A. Rae, T. King, J. G. Chichorro, Blockade of endothelin receptors reduces tumor-induced ongoing pain and evoked hypersensitivity in a rat model of facial carcinoma induced pain, Eur. J. Pharm. 818 (2018) 132–140.
[16] S. Bhalla, S.V. Andurkar, A. Gulati, Neurobiology of opioid withdrawal: role of the endothelin system, Life Sci. 159 (2016) 34–42.
[17] P.N. Quang, B.L. Schmidt, Endothelin-A receptor antagonism attenuates carcinoma-induced pain through opioids in mice, J. Pain 11 (7) (2010) 663–671.
[18] L. Mazzardo-Martins, D.C. Salm, E.C. Winkelmann-Duarte, J.K. Ferreira, D. D. Ludtke, K.P. Frech, L.A.O. Belmonte, V.V. Horewicz, A.P. Piovezan, F.J. Cidral-Filho, A.O.O. More, D.F. Martins, Electroacupuncture induces antihyperalgesic effect through endothelin-B receptor in the chronic phase of a mouse model of complex regional pain syndrome type I, Pflug Arch. 470 (12) (2018) 1815–1827.
[19] X. Chen, Z. Zhai, K. Huang, W. Xie, J. Wan, C. Wang, Bosentan therapy for pulmonary arterial hypertension and chronic thromboembolic pulmonary hypertension: A systemic review and meta-analysis, Clin. Respir. J. 12 (6) (2018) 2065–2074.
[20] S. Bhalla, G. Matwyshyn, A. Gulati, Potentiation of morphine analgesia by BQ123, an endothelin antagonist, Peptides 23 (10) (2002) 1837–1845.
[21] S. Bhalla, G. Matwyshyn, A. Gulati, Endothelin receptor antagonists restore morphine analgesia in morphine tolerant rats, Peptides 24 (4) (2003) 553–561.
[22] S. Bhalla, G. Pais, M. Tapia, A. Gulati, Endothelin ETA receptor antagonist reverses naloxone-precipitated opioid withdrawal in mice, Can. J. Physiol. Pharm. 93 (11) (2015) 935–944.
[23] K.A. Jacobson, New paradigms in GPCR drug discovery, Biochem. Pharm. 98 (4) (2015) 541–555.
[24] M.A. Ayoub, Y. Zhang, R.S. Kelly, H.B. See, E.K. Johnstone, E.A. McCall, J. H. Williams, D.J. Kelly, K.D. Pfleger, Functional interaction between angiotensin II receptor type 1 and chemokine (C-C motif) receptor 2 with implications for chronic kidney disease, PLoS One 10 (3) (2015), 0119803.
[25] M. Le Naour, M.M. Lunzer, M.D. Powers, A.E. Kalyuzhny, M.A. Benneyworth, M. J. Thomas, P.S. Portoghese, Putative kappa opioid heteromers as targets for developing analgesics free of adverse effects, J. Med. Chem. 57 (15) (2014) 6383–6392.
[26] A. Gupta, F.M. Decaillot, L.A. Devi, Targeting opioid receptor heterodimers: strategies for screening and drug development, AAPS J. 8 (1) (2006) E153–E159.
[27] L. Zhang, J.T. Zhang, L. Hang, T. Liu, Mu opioid receptor heterodimers emerge as novel therapeutic targets: recent progress and future perspective, Front. Pharmacol. 11 (2020) 1078.
[28] I. Gomes, A. Gupta, J. Filipovska, H.H. Szeto, J.E. Pintar, L.A. Devi, A role for heterodimerization of mu and delta opiate receptors in enhancing morphine analgesia, Proc. Natl. Acad. Sci. U.S.A. 101 (14) (2004) 5135–5139.

[29] E. Erbs, L. Faget, G. Scherrer, A. Matifas, D. Filliol, J.L. Vonesch, M. Koch, P. Kessler, D. Hentsch, M.C. Birling, M. Koutsourakis, L. Vasseur, P. Veinante, B. L. Kieffer, D. Massotte, A mu-delta opioid receptor brain atlas reveals neuronal co-occurrence in subcortical networks, Brain Struct. Funct. 220 (2) (2015) 677–702.
[30] S. Angers, A. Salahpour, M. Bouvier, Dimerization: an emerging concept for G protein-coupled receptor ontogeny and function, Annu. Rev. Pharm. Toxicol. 42 (2002) 409–435.
[31] M. Hojo, Y. Sudo, Y. Ando, K. Minami, M. Takada, T. Matsubara, M. Kanaide, K. Taniyama, K. Sumikawa, Y. Uezono, mu-Opioid receptor forms a functional heterodimer with cannabinoid CB1 receptor: electrophysiological and FRET assay analysis, J. Pharm. Sci. 108 (3) (2008) 308–319.
[32] B.A. Jordan, I. Gomes, C. Rios, J. Filipovska, L.A. Devi, Functional interactions between mu opioid and alpha 2A-adrenergic receptors, Mol. Pharm. 64 (6) (2003) 1317–1324.
[33] Eisai R&D Management Co Ltd, T. Keigo, N. Tomoki, Sitaxentan derivative/US8592470B2, https://patents.google.com/patent/US8592470B2/en (Accessed 26 November 2013).
[34] K. Miyano, Y. Sudo, A. Yokoyama, K. Hisaoka-Nakashima, N. Morioka, M. Takebayashi, Y. Nakata, Y. Higami, Y. Uezono, History of the G protein-coupled receptor (GPCR) assays from traditional to a state-of-the-art biosensor assay, J. Pharm. Sci. 126 (4) (2014) 302–309.
[35] S. Manabe, K. Miyano, Y. Fujii, K. Ohshima, Y. Yoshida, M. Nonaka, M. Uzu, Y. Matsuoka, T. Sato, Y. Uezono, H. Morimatsu, Possible biased analgesic of hydromorphone through the G protein-over beta-arrestin-mediated pathway: cAMP, CellKey, and receptor internalization analyses, J. Pharm. Sci. 140 (2) (2019) 171–177.
[36] H. Sakairi, Y. Kamikubo, M. Abe, K. Ikeda, A. Ichiki, T. Tabata, M. Kano, T. Sakurai, G protein-coupled glutamate and GABA receptors form complexes and mutually modulate their signals, ACS Chem. Neurosci. 11 (4) (2020) 567–578.
[37] F.H. Mujenda, A.M. Duarte, E.K. Reilly, G.R. Strichartz, Cutaneous endothelin-a receptors elevate post-incisional pain, Pain 133 (1–3) (2007) 161–173.
[38] V. Pickering, R. Jay Gupta, P. Quang, R.C. Jordan, B.L. Schmidt, Effect of peripheral endothelin-1 concentration on carcinoma-induced pain in mice, Eur. J. Pain. 12 (3) (2008) 293–300.
[39] A. Furukawa, M. Shinoda, A. Kubo, K. Honda, R. Akasaka, Y. Yonehara, K. Iwata, Endothelin signaling contributes to modulation of nociception in early-stage tongue cancer in rats, Anesthesiology 128 (6) (2018) 1207–1219.
[40] X.B. Yan, T.C. Peng, D. Huang, Correlations between plasma endothelin-1 levels and breakthrough pain in patients with cancer, Onco Targets Ther. 8 (2015) 3703–3706.
[41] M. Ihara, K. Noguchi, T. Saeki, T. Fukuroda, S. Tsuchida, S. Kimura, T. Fukami, K. Ishikawa, M. Nishikibe, M. Yano, Biological profiles of highly potent novel endothelin antagonists selective for the ETA receptor, Life Sci. 50 (4) (1992) 247–255.
[42] P. Tewson, S. Martinka, N. Shaner, C. Berlot, A.M. Quinn, T. Hughes, Assay for detecting galphai-mediated decreases in cAMP in living cells, SLAS Discov. 23 (9) (2018) 898–906.
[43] A. Manglik, H. Lin, D.K. Aryal, J.D. McCorvy, D. Dengler, G. Corder, A. Levit, R. C. Kling, V. Bernat, H. Hubner, X.P. Huang, M.F. Sassano, P.M. Giguere, S. Lober, D. Da, G. Scherrer, B.K. Kobilka, P. Gmeiner, B.L. Roth, B.K. Shoichet, Structure-based discovery of opioid analgesics with reduced side effects, Nature 537 (7619) (2016) 185–190.
[44] D.G. Soergel, R.A. Subach, N. Burnham, M.W. Lark, I.E. James, B.M. Sadler, F. Skobieranda, J.D. Violin, L.R. Webster, Biased agonism of the mu-opioid receptor by TRV130 increases analgesia and reduces on-target adverse effects versus morphine: a randomized, double-blind, placebo-controlled, crossover study in healthy volunteers, Pain 155 (9) (2014) 1829–1835.
[45] S. Bhalla, G. Matwyshyn, A. Gulati, Morphine tolerance does not develop in mice treated with endothelin-a receptor antagonists, Brain Res. 1064 (1–2) (2005) 126–135.
[46] S.M. Rawls, K. Benamar, Effects of opioids, cannabinoids, and vanilloids on body temperature, Front. Biosci. Sch. Ed. 3 (2011) 822–845.
[47] P. Salmi, J. Kela, U. Arvidsson, C. Wahlestedt, Functional interactions between delta- and mu-opioid receptors in rat thermoregulation, Eur. J. Pharm. 458 (1–2) (2003) 101–106.
[48] A. Serrano, M.A. Aguilar, C. Manzanedo, M. Rodriguez-Arias, J. Minarro, Effects of DA D1 and D2 antagonists on the sensitisation to the motor effects of morphine in mice, Prog. Neuropsychopharmacol. Biol. Psychiatry 26 (7–8) (2002) 1263–1271.
[49] R. Benyamin, A.M. Trescot, S. Datta, R. Buenaventura, R. Adlaka, N. Sehgal, S. E. Glaser, R. Vallejo, Opioid complications and side effects, Pain Physician 11 (2 Suppl) (2008) S105–S120.
[50] G.A. Matwyshyn, S. Bhalla, A. Gulati, Endothelin ETA receptor blockade potentiates morphine analgesia but does not affect gastrointestinal transit in mice, Eur. J. Pharm. 543 (1–3) (2006) 48–53.